

Phase Retrieval of Elongated Laser Guide Star by Sphere Packing Coded Apertures

Bastián Romero^a, Nelson Díaz^a, Jorge Tapia^a, and Esteban Vera^a

^aPontificia Universidad Católica de Valparaíso, Brasil 2147, 2362804 Valparaíso.

ABSTRACT

The new generation of extremely large telescope (ELT) introduces many challenges in optics and engineering. A key challenge is the development of an adaptive optics system able to handle elongated laser guide star (ELGS). Classic wavefront sensor (WFS), such as the shack-hartmann wavefront sensor (SHWFS) or pyramidal wavefront sensor (PyWFS), are not able to readily handle elongated stars, which gets worse when the atmospheric turbulence becomes stronger. In this work, we present a novel complex field wavefront sensor (CFWFS) that can reconstruct the phase and amplitude of the extended bodies at the image plane, and then it is able to recover the turbulent phase at the pupil plane. The proposed WFS scheme uses a four times faster parallel phase retrieval algorithm with only eight designed coded aperture (DCA) that is designed using sphere packing coded apertures (SPCA). We present a collection of encouraging preliminary simulation results.

Keywords: phase retrieval, elongated laser guide star, wavefront sensor, designed coded aperture, sphere packing.

1. INTRODUCTION

Phase retrieval (PR) is a technique that recovers a complex-valued signal from intensity-only measurements, whose applications span from X-ray crystallography¹ to adaptive optics (AO).² Precisely, AO measures the phase of a reference star using a wavefront sensor (WFS) and compensates for the phase distortion using an adaptive mirror.³ Examples of WFS include the conventional shack-hartmann wavefront sensor (SHWFS)⁴ and the pyramidal wavefront sensor (PyWFS).⁵ However, applying AO in the new generation of giant telescopes is a significant challenge for conventional WFS because the laser guide star (LGS) introduces perspective issues when interacting with the sodium layer given the massive aperture of the ELTs, and even state-of-the-art WFSs⁶ are not able to handle them.

Fig. 1(a) illustrates the profile of an LGS that shows the effects due to the perspective, which results in an elongated and cylindrical volume as shown in Fig. 1(b), hereinafter referred to as an elongated laser guide star (ELGS). The thickness of an ELGS is approximately 20 km at approximately 90 km above sea level, with a width of one arcsecond. In the case of the PyWFS, in the perfect case, the intensity is the same for the four pupils, but for ELGS, the four pupils exhibit a non-uniform intensity.⁷ In the case of the SHWFS, each lens of the microlens array must produce a spot in the sensor, but the perspective of the ELGS modifies this, and the light in the sensor loses the spot form, instead showing tilted spots.⁸

To address these challenges, in this work, we propose a complex field wavefront sensor (CFWFS), which has the spatial resolution to measure the phase and amplitude generated by the extended bodies at the image plane under strong atmospheric turbulence in the scenario where the reference star is elongated. This novel WFS uses a designed coded aperture (DCA) based on sphere packing (SP)⁹ to accelerate the convergence of the phase retrieval (PR) relying only on a set of intensity measurements and an sparse recovery algorithms to obtain low-order Zernikes of the turbulence at the pupil plane.¹⁰⁻¹²

E-mail: bastian.romero@pucv.cl

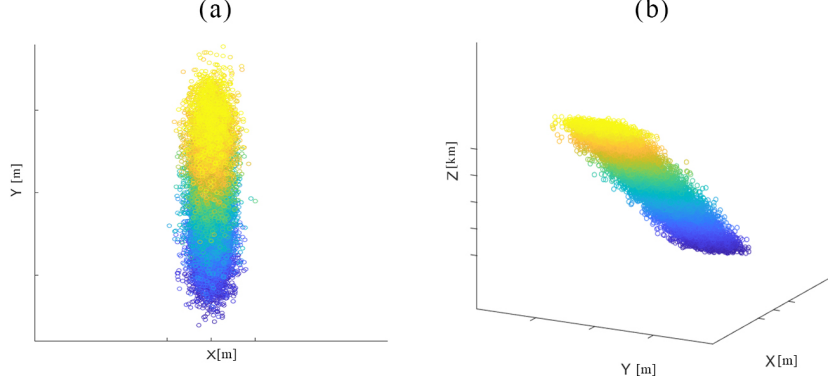


Figure 1. Three-dimensional representation of ELGS (a) x-y profile (b) perspective of the ELGS.

2. METHOD

2.1 Proposed optical wavefront sensing of elongated reference star

Fig. 2 shows the acquisition and inference steps of the proposed optical wavefront sensing for a telescope. The scheme of the proposed optical WFS that measures an elongated reference star is depicted in Fig. 2(a). The phase information of the telescope pupil plane (TPP), represented in Fig. 2(b), is propagated through a $4f$ -system with a specific magnification, where the amplitude and phase depicted in Fig. 2(c) is imaging at the focal plane between the two lenses that comprise it. The goal of this $4f$ -system is to generate a conjugate telescope pupil plane (CTPP), place where it is superimposed with the information of a specific CA, such as those depicted in Fig. 2(d). Finally, the encoded light in CTPP is propagated a distance z up to the sensor, generating the necessary information to obtain the phase of the ELGS with PR algorithm, as is shown in Fig. 2(e). When the reconstructed phase is computed, this phase is backwards propagated to the pupil plane to correct the turbulent phase. Finally, the phase in the pupil plane is decomposed into Zernike modes by the least absolute shrinkage and selection operator (LASSO).

2.2 Phase Retrieval Forward Model

PR is a method for measuring the phase of a signal through the relation between the image and its Fourier plane¹³ and refers to Fresnel or Fraunhofer propagation. In this research, we use Fresnel propagation to generate the compressed measurement (CM) in the sensor.¹⁴ Numerous strategies exist for creating diverse diffraction patterns, including using different planes and shifting the object.^{15,16} We use coded illumination (CI) to obtain the CMs in the sensor. The forward model of the acquired CMs is given by

$$\mathbf{Y}_\ell = |P(z) \{\mathbf{A}_\ell \odot \mathbf{O}\}|^2, \quad (1)$$

where $\mathbf{Y}_\ell \in \mathbb{R}^{d \times d}$ is the ℓ^{th} CM in the sensor, such that $d \times d$ is the number of pixels in the detector, $\mathbf{A}_\ell \in \{0, 1\}^{d \times d}$ is the ℓ^{th} binary coded aperture (CA) and \odot denotes the Hadamard product, $\mathbf{O} \in \mathbb{C}^{d \times d}$ is the complex object that has the hidden phase, $P(z)$ represents the near-field propagation model, z is the propagation distance between the object plane and the sensor and $|\cdot|$ is the element-wise modulus operator. Leveraging the unique and uniform sampling of the SPCA, the underlying phase can be recovered by solving a tensor completion problem by assuming a low rank. The resulting forward model is expressed as a linear model

$$\mathbf{y} = |\langle \mathbf{H}, \mathbf{x}, \phi \rangle|^2 + \boldsymbol{\omega}, \quad (2)$$

where $\mathbf{y} \in \mathbb{R}^m$ is the CM in the plane propagation ϕ , $\mathbf{H} \in \{0, 1\}^{m \times n}$ is the sensing matrix, with $m \gg n$, $\boldsymbol{\omega}$ is the additive noise, and $\mathbf{x} \in \mathbb{C}^n$, is the hidden phase. To recover \mathbf{x} from the set CM \mathbf{y} , we assume that \mathbf{x} is the phase of object \mathbf{O} with a well-known intensity and hidden phase.¹⁷

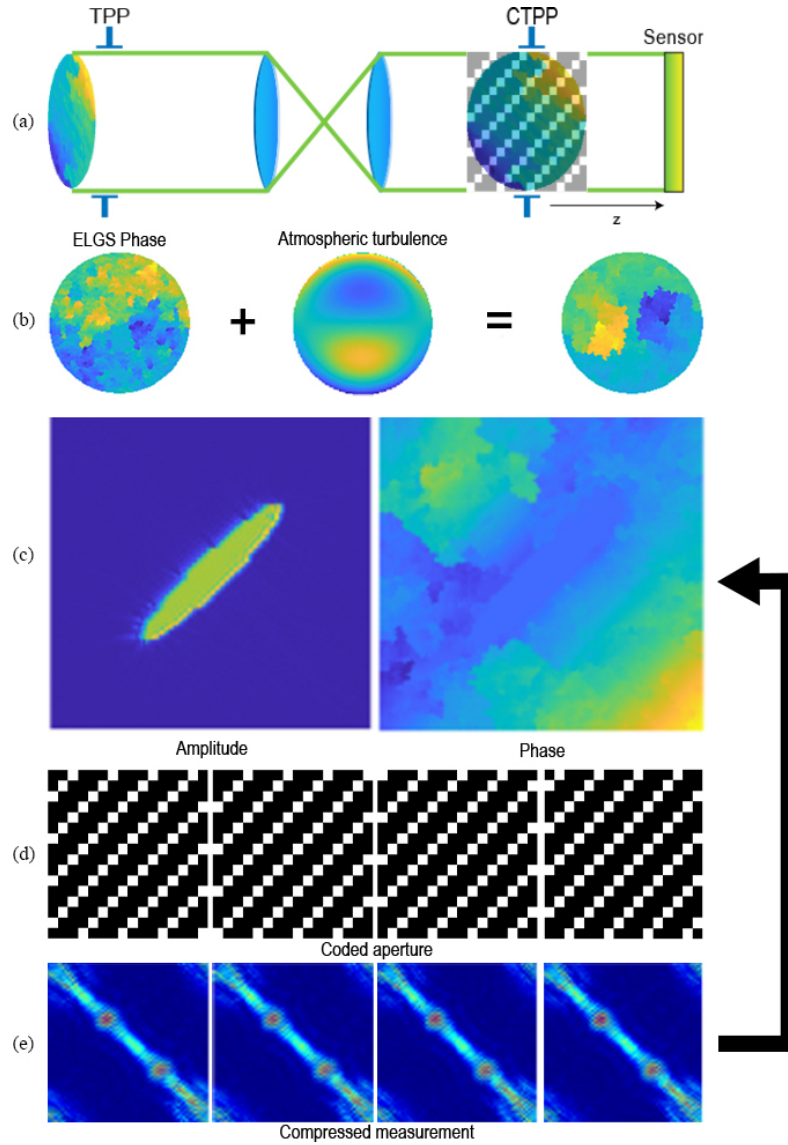


Figure 2. (a) General scheme of AO with ELGS; (b) linear combination of atmospheric turbulence and phase of elongated reference star in the sky; (c) reconstructed complex object; (d) CAs; (e) CM in the sensor.

3. SIMULATION

We simulate to demonstrate the advantages of our SPCA approach. This simulation considers a 128×128 pixel size sensor, and the simulation only uses eight CAs to measure the eight CMs and leverages the matrix completion method to reconstruct the phase faster by exploiting uniform sampling because each pixel is sampled only twice. The transmittance in our SPCA approach is 25%. Two key advantages of our method are the uniform sampling and the fast reconstruction. We use an ellipse under different rotations to simulate a ELGS. Fig. 3 shows the simulation data, Fig. 3(a) shows the groundtruth of ELGS, the amplitude is rotated by 45, 90 and -45 degrees to simulate the different conditions of ELGS, and the phase is the linear combination of tilt and vertical coma Zernikes. Fig. 3(b-e) shows the amplitude reconstruction with different rotations at the top, and at the bottom, the phase reconstruction and Fig. 3(f) shows the Zernike coefficients and modes. The orange bar is the groundtruth and the blue bar is the reconstruction. This shows that phase reconstruction is similar to the groundtruth, giving greater importance to tilt and vertical coma. Fig. 4 shows the result with strong simulated turbulence. Fig. 4(a) shows the phase groundtruth at the bottom. In this case, the Zernike modes shown in Fig. 4(f) are similar in certain modes such as tilt, tip and vertical trefoil; all modes correspond to low-order Zernike. The phase reconstruction at the bottom of Fig. 4(b-e) is a low-order reconstruction with the main components of the Zernike modes.

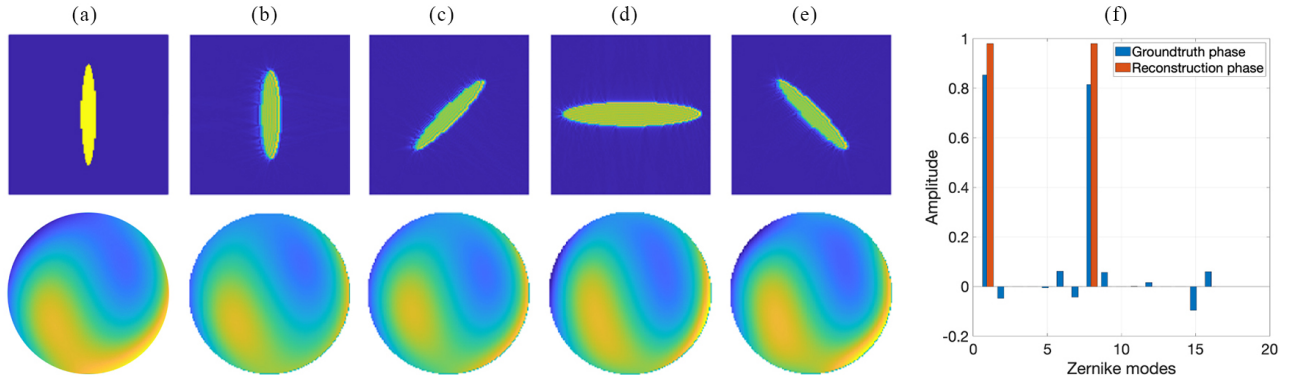


Figure 3. Complex object reconstruction of a ELGS with (a) amplitude groundtruth and a linear combination of tilt and vertical coma as phase groundtruth, using amplitude rotations of (b) 0, (c) 45, (d) 90 and (e) -45 degrees; (f) weight of the Zernike modes.

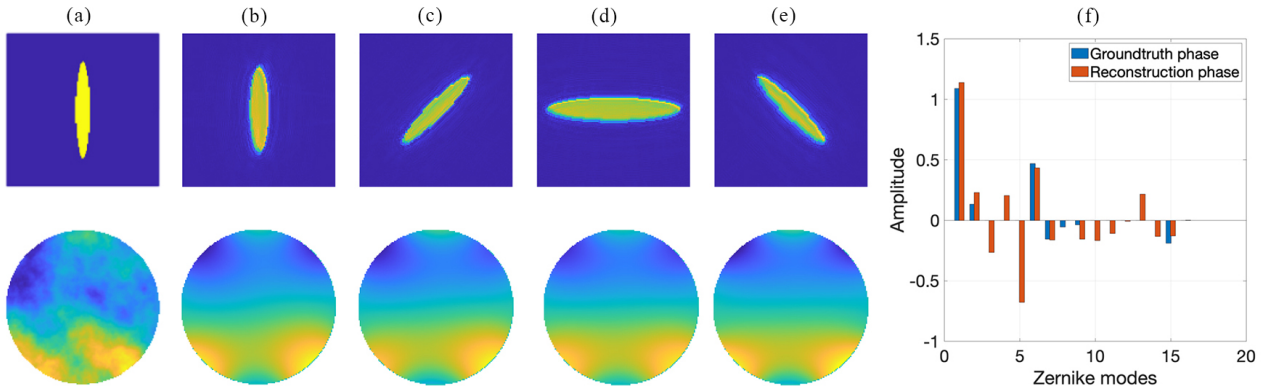


Figure 4. Complex object reconstruction of a ELGS with (a) amplitude groundtruth and simulated strong turbulence as phase groundtruth, using amplitude rotations of (b) 0, (c) 45, (d) 90 and (e) -45 degrees; (f) weight of the Zernike modes.

4. CONCLUSION

We introduce a novel wavefront sensor that leverages the uniform sensing of sphere packing coded apertures to recover the underlying phase and amplitude of the elongated reference star, and hence the turbulent phase at the pupil plane, using phase retrieval and tensor completion. We perform extensive simulations using our SPCA. Furthermore, the simulation of the complex field wavefront sensor demonstrates that our approach exploits the sparsity of the recovered phase at the pupil plane to filter out components that may belong to the extended object. In future work, we plan to extend our wavefront sensing scheme for elongated reference star by replacing the SPCA with complementary coded apertures, which has been proven successful in retrieving the phase and amplitude using complementary Hadamard coded apertures.¹⁸

ACKNOWLEDGMENTS

This work was supported in part by Agencia Nacional de Investigación y Desarrollo (ANID) under grants ANILLO ATE220022, QUIMAL 220006, MAGISTER NACIONAL 2022-22220809, and FONDECYT Postdoctorado 3220561 and FONDECYT Postdoctorado 3230489.

REFERENCES

- [1] Millane, R. P., “Phase retrieval in crystallography and optics,” *J. Opt. Soc. Am. A* **7**, 394–411 (Mar 1990).
- [2] Gonsalves, R. A., “Phase retrieval and diversity in adaptive optics,” *Optical Engineering* **21**(5), 829–832 (1982).
- [3] Roddier, F., “Adaptive optics in astronomy,” (1999).
- [4] Merkle, F., “Adaptive optics,” *Physics World* **4**(1), 33 (1991).
- [5] Ragazzoni, R., “Pupil plane wavefront sensing with an oscillating prism,” *Journal of Modern Optics* **43**(2), 289–293 (1996).
- [6] Ragazzoni, R., Farinato, J., and Marchetti, E., “Adaptive optics for 100-m-class telescopes: new challenges require new solutions,” in [*Adaptive Optical Systems Technology*], **4007**, 1076–1087, SPIE (2000).
- [7] Oyarzún, F., Chambouleyron, V., Neichel, B., Fusco, T., and Guesalaga, A., “Expected performance of the pyramid wavefront sensor with a laser guide star for 40 m class telescopes,” *Astronomy & Astrophysics* **686**, A1 (2024).
- [8] Basden, A. G., Chemla, F., Dipper, N., Gendron, E., Henry, D., Morris, T., Rousset, G., and Vidal, F., “Real-time correlation reference update for astronomical adaptive optics,” *Monthly Notices of the Royal Astronomical Society* **439**, 968–976 (01 2014).
- [9] Diaz, N., Alvarado, A., Meza, P., Guzmán, F., and Vera, E., “Multispectral filter array design by optimal sphere packing,” *IEEE Transactions on Image Processing* **32**, 3634–3649 (2023).
- [10] Fienup, J. R., “Reconstruction of an object from the modulus of its fourier transform,” *Optics letters* **3**(1), 27–29 (1978).
- [11] Candes, E. J., Eldar, Y. C., Strohmer, T., and Voroninski, V., “Phase retrieval via matrix completion,” *SIAM review* **57**(2), 225–251 (2015).
- [12] Smith, J. S., “Iterative transform phase diversity: An object and wavefront recovery algorithm,” in [*Frontiers in Optics*], FThK2, Optica Publishing Group (2011).
- [13] Gerchberg, R. W., “A practical algorithm for the determination of plane from image and diffraction pictures,” *Optik* **35**(2), 237–246 (1972).
- [14] Schmidt, J., [*Numerical simulation of optical wave propagation: With examples in MATLAB*] (01 2010).
- [15] Pedrini, G., Osten, W., and Zhang, Y., “Wave-front reconstruction from a sequence of interferograms recorded at different planes,” *Optics letters* **30**(8), 833–835 (2005).
- [16] Gao, P., Pedrini, G., and Osten, W., “Phase retrieval with resolution enhancement by using structured illumination,” *Optics Letters* **38**(24), 5204–5207 (2013).
- [17] Guerrero, A., Pinilla, S., and Arguello, H., “Phase recovery guarantees from designed coded diffraction patterns in optical imaging,” *IEEE Transactions on Image Processing* **29**, 5687–5697 (2020).
- [18] Romero, B., Cofré, A., Diaz, N., Scherz, P., Tapia, J., Peters, E., Perez, D., and Vera, E., “Phase Retrieval by Designed Hadamard Complementary Coded Apertures.,” *Optica Open* (2024).